Engineering Analysis with Boundary Elements 35 (2011) 517–526

Contents lists available at ScienceDirect

Engineering Analysis with Boundary Elements

journal homepage: www.elsevier.com/locate/enganabound

# Constructing efficient substructure-based preconditioners for BEM systems of equations ☆

F.C. de Araújo [a],*, E.F. d'Azevedo [b], L.J. Gray [b]

[a] Department of Civil Eng., UFOP, 35400-000 Ouro Preto-MG, Brazil
[b] Computer Science and Math. Div., ORNL, Oak Ridge, P.O. Box 2008, USA

ARTICLE INFO

*Article history:*
Received 11 March 2010
Accepted 13 August 2010
Available online 14 October 2010

*Keywords:*
3D boundary-element models
Subregion-by-subregion algorithm
Krylov solvers
Substructure-based block-diagonal preconditioners

ABSTRACT

In this work, a generic substructuring algorithm is employed to construct global block-diagonal preconditioners for BEM systems of equations. In this strategy, the allowable fill-in positions are those on-diagonal block matrices corresponding to each BE subregion. As these subsystems are independently assembled, the preconditioner for a particular BE model, after the **LU** decomposition of all subsystem matrices, is easily formed. So as to highlight the efficiency of the preconditioning proposed, the Bi-CG solver, which presents a quite erratic convergence behavior, is considered. In the particular applications of this paper, 3D representative volume elements (RVEs) of carbon-nanotube (CNT) composites are analyzed. The models contain up to several tens of thousands of degrees of freedom. The efficiency and relevance of the preconditioning technique is also discussed in the context of developing general (parallel) BE codes.

## 1. Introduction

Applying iterative solvers to large-order engineering problems has been intensively pursued in the last decades, mainly because their unquestionable appeal to solve truly large models [1,2]. Herein, the parallelism embedded in them allied with the today's parallel computer architectures plays a decisive role, so that it can be well stated that developing fast scalable (preconditioned) parallel Krylov solvers is a key point for getting high-fidelity solution for large-order complex engineering problems. In these cases, direct solvers may be exceedingly expensive concerning both memory and CPU time, and their parallel implementation is awkward.

For general non-symmetric matrices, like BE matrices, based on the number of terms involved in the iterative formulas, the Krylov solvers can be subdivided in two broad classes of algorithms: long-recurrence algorithms (GMRES and variants) and short-recurrence ones (Bi-CG and variants). Over the last several decades, milestone contributions in these algorithms have been definitely given by the following works: the Lanczos method (by Lanczos in 1952) [3], the Bi-CG method (by Fletcher in 1976) [4], the GMRES method (by Saad and Schultz in 1986) [5], the CGS method (by Sonneveld in 1989) [6], the Bi-CGSTAB (by van der Vosrt in 1992) [7], and the Bi-CGSTAB($l$) (by Sleijpen and Fokkema in 1993) [8]. Of course, in this period of time, a series of other works that significantly contributed for increasing the efficiency of Krylov solvers have also been published, including those related to particular applications to symmetric definite matrices.

Particularly for BEM systems of equations, the first successful applications of iterative solvers were reported at the end of the 80s and beginning of the 90s [9–12], wherein diagonal-preconditioned Bi-CG [9–10,12], and preconditioned GMRES [11] methods were used. According to the authors' knowledge, before these works, only basic iterative methods as the Jacobi or Gauss–Seidel methods, or at most the CGN solver, which consists of applying the CG method to the normal equations, $\mathbf{A}^T\mathbf{A}\mathbf{x}=\mathbf{A}^T\mathbf{b}$, had been considered [13–14]. A patent disadvantage of these iterative solvers are the non-reliability regarding convergence, so that they actually cannot be regarded as general-purpose solvers for practical applications. In fact, applying basic iterative methods, convergence is assured only if the spectral radius of the corresponding iteration matrix is less than 1, which is not the case for general systems. On the other hand, considering the CGN has the disadvantage of squaring the condition number of the original system $\mathbf{A}\mathbf{x}=\mathbf{b}$, which may cause the iterative process fail to converge. The Bi-CG and GMRES methods, and their variants (or combinations) are then the remaining alternatives for deriving general-purpose solvers for BEM equations.

In fact, long-term recurrence methods as GMRES and variants should be avoided because of memory requirements for large problems and non-rare convergence stagnation in practice.

☆ Sponsors: Brazilian Research Council, CNPq; Research Foundation of the State of Minas Gerais, FAPEMIG; Office of Advanced Scientific Computing Research, U.S. Department of Energy.

* Corresponding author. Tel.: +55 31 3559 1468; fax: +55 31 3559 1548.
*E-mail addresses:* fcelio@em.ufop.br (F.C. de Araújo), dazevedoef@ornl.gov (E.F. d'Azevedo), graylj1@ornl.gov (L.J. Gray).

0955-7997/$ - see front matter © 2010 Elsevier Ltd. All rights reserved.
doi:10.1016/j.enganabound.2010.09.001

Restarting the iterative process after a number $m$ of iterations is an obvious strategy for reducing memory costs involved in using GMRES, but, depending on the choice of $m$, bad convergence characteristics (including stagnation) may be enhanced, also leading to non-reliable solvers for general purposes in practice. Concerning the Bi-CG method, the shortcoming is its erratic convergence behavior. Thus, a likely optimal iterative solver should be generated by combining the Bi-CG method, which takes into account short-term recurrences, with a residual-minimization method, as the GMRES, which should smooth out convergence irregularities connected with the Bi-CG iterations. Following these ideas culminated in developing the transpose-free Bi-CGSTAB($l$) [8] and the GPBi-CG (generalized product Bi-CG) [15] solvers.

Whether or not solvers like the Bi-CGSTAB($l$) or the GPBi-CG will always, sure and fast, provide an accurate solution for any practical problem, it is a question that does not have any mathematically founded answer yet. However, two facts are relevant herein. First, convergence failure or slowness is a token that the corresponding model is not suitable for the description of the physical response; second, preconditioners may be employed to accelerate the iterative process [1,17]. For BEM solvers, a series of preconditioners have been reported in the technical literature [9–12,16–19,20]. In general, the splitting matrix of basic iterative methods as the Jacobi, block Jacobi, Gauss–Seidel or incomplete **LU** decomposition methods can be used to construct preconditioners. Roughly speaking, preconditioners are also a way to state a relationship between direct and iterative solvers, in the sense that if the preconditioning matrix becomes the system matrix, so the iterative method at hand becomes a direct solver (giving then the system solution at one single iteration step). Furthermore, domain decomposition methods (DDM) allied with direct methods may also be employed to construct global preconditioners. Herein, in general, direct solvers are employed to get the solution for the many subdomains, while iterative techniques describe the interactions between them. Concerning the parallel processing (actually not addressed in this study), we see that domain decomposition strategies also suits to easily parallelize incomplete **LU**-based preconditioners, indeed the most efficient ones, but not easily parallelizable. In case of block-diagonal preconditioners, the parallelization is straightforward. Thus, DDM-based preconditioners are very convenient for developing parallel solvers.

In this work, we objectively employ the BE substructuring algorithm [21–22] to form a global block-diagonal preconditioner. This substructuring algorithm is nothing other than a DDM-based strategy to decompose a certain problem domain into a generic number of coupled BE models, so that the preconditioning here developed can be designated as a BE-subdomain-based preconditioner. Although the coupling conditions between the subdomains are imposed in a direct (non-iterative) way, the subsystems are independently assembled, and so the block-diagonal matrices corresponding to each subregion can be easily decomposed in their **L** and **U** factors. It is worth commenting that the price paid for constructing this preconditioning, which is much higher than e.g. a plain diagonal one, is in fact insignificant if convergence reliability and convenience for developing general parallel boundary-element codes is attained. Moreover, the more the number of subregions, the less expensive the constructing of the BE-substructuring-based preconditioner is. For the applications here, the preconditioning proposed is incorporated into the Bi-CG solver. As this solver is theoretically less efficient than the Bi-CGSTAB($l$) or the GPBi-CG solvers, as discussed above, the efficiency of the preconditioner itself will be highlighted in the numerical experiments.

This paper is structured in the following way: we present an overview of the generic BE substructuring algorithm in Section 2, the construction of the preconditioner in Section 3, and analyze different complex carbon-nanotube (CNT) composites in Section 4. The models considered contains up to several tens of thousands of degrees of freedom. The efficiency and relevance of the preconditioning proposed is discussed also in the context of ideas for developing general scalable BE parallel codes, in effect the goal of the chief ideas on the base of this paper.

## 2. The boundary-element substructuring algorithm

The fact that the boundary element method (BEM) is derived from the exact boundary-integral representation of problem solutions, in closed or open domains, accounts for the following advantages: high accuracy, fulfillment of radiation conditions in open domains, and easier mesh generation. Indeed, very accurate responses are obtained if homogeneous single-domain problems are considered and the integrals involved are accurately evaluated. However, this is way not the case in practice, wherein e.g. material heterogeneity is often present, and a BE subregion technique is in general needed. Here, the BE subregion-by-subregion (BE-SBS) algorithm reported in Refs. [21,22] is adopted to both model complex heterogeneous problems as CNT composites, and to construct preconditioners to be used together with the Krylov solver embedded.

To derive the BE-SBS algorithm, besides continuous elements, discontinuous boundary elements are employed when needed. Herein, another interesting characteristic of the BEM is taken into account: interelement compatibility (in the FE sense) is not required to assure solution convergence. Actually, discontinuous elements allow generating very complex boundary-element models, for instance containing a number of inclusions and voids as in composites. If only continuous boundary elements were used, setting up complex coupled models for general problems may be awkward [23]. Thus, considering discontinuous boundary elements is very convenient. However, because of the unavoidable proximity of the displaced collocation (functional) nodes to neighboring elements (see Fig. 1), besides singular, nearly singular integrals also take place, and special quadratures are required.

As known, in 3D elasticity standard boundary-element formulations, surface integrals of the form

$$\int_{\Gamma_e} p^*_{ik}(\chi;\xi)u_i(\chi)\mathrm{d}\Gamma(\chi), \tag{1a}$$

$$\int_{\Gamma_e} u^*_{ik}(\chi;\xi)p_i(\chi)\mathrm{d}\Gamma(\chi), \tag{1b}$$

take place, where $u^*_{ik}$ and $p^*_{ik}$ are the Kelvin fundamental kernels, $u_i$ and $p_i$ the boundary displacement and traction, respectively, and $\Gamma_e$ the surface of the $e$th boundary. Actually, the efficient evaluation of these integrals in the singular and nearly singular

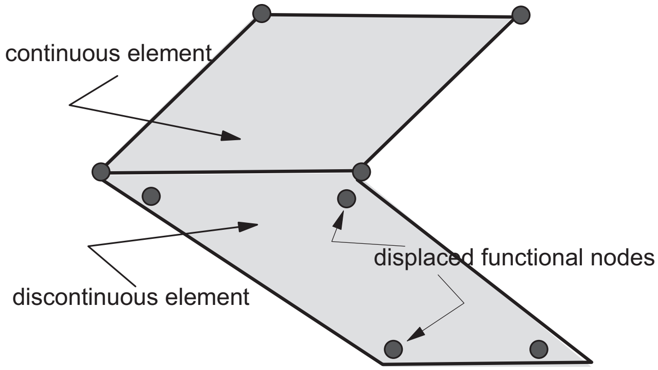

**Fig. 1.** Discontinuous boundary elements.

cases is needed for getting high-quality responses. In previous works [21,22,24–28], several numerical quadratures have been investigated. One has concluded that the numerical integration strategy proposed in Ref. [22] was the best one among the techniques observed. It has the following characteristics:

1. Weakly singular and nearly weakly singular surface integrals are computed by combining triangle-polar [24] and polynomial coordinate transformations [25];
2. Nearly strongly singular integrals are evaluated by applying the line-integral approach reported in Refs. [26,27] together with the improvements brought about in Ref. [22], which concern the inclusion of analytical expressions for nearly strongly singular line integrals occurring in the process.
3. Strongly singular integrals (Cauchy principal values) are indirectly calculated by applying rigid-body displacements.

In the above, the terms *nearly weakly singular* and *nearly strongly singular integrals* mean a nearly singular integral associated, respectively, with $u_{ik}^{*}$ (the weakly singular kernel) and $p_{ik}^{*}$ (the strongly singular kernel). All details of the quadratures involved are described in Ref. [22]. Of course, this integration strategy also suits to model thin-walled domains, allowing then e.g. the modeling of shell-like elements by means of 3D formulations.

With proper integration procedures, discontinuous boundary elements can be used, and so the BE-SBS algorithm, reported in Refs. [21,22], is derived. This algorithm is comparable to the element-by-element (EBE) technique, developed to finite-element analysis

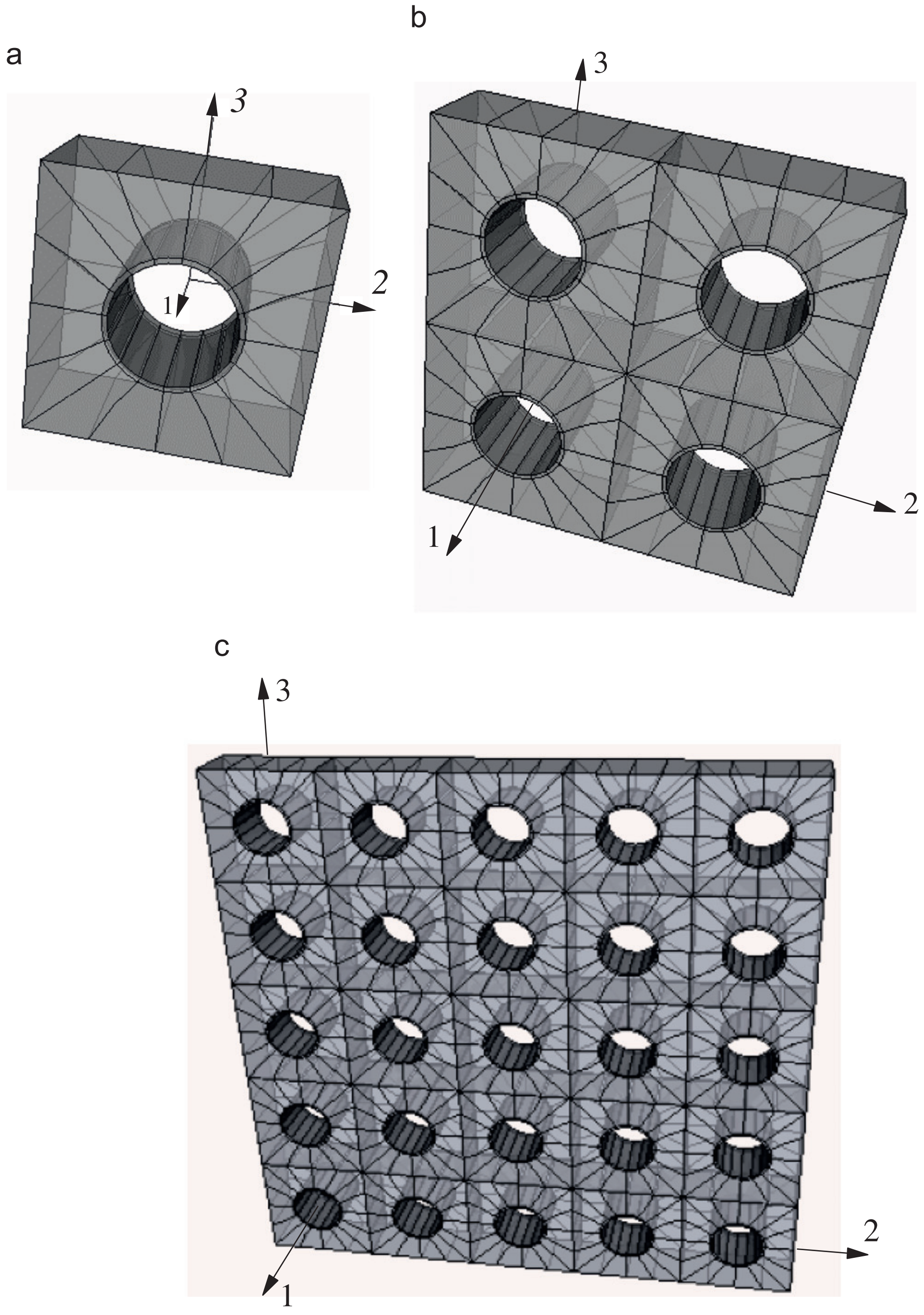

**Fig. 2.** Square-packed long-CNT-based RVEs.

(FEA) [29] while a subregion or substructure corresponds to a finite element. Notice that, if needed, we could have a subregion mesh as fine as a finite-element mesh, and if the BE global system matrix were explicitly assembled, it would be highly sparse as well. Furthermore, the BE-SBS algorithm can also be compared to finite element tearing and interconnecting (FETI) methods [30], where a given problem domain is decomposed (torn) into non-overlapping subdomains and posteriorly interconnected by imposing the corresponding continuity conditions at the interfaces.

Unlike other BE–BE coupling algorithms which look for suitable compressed formats to store the corresponding global sparse matrix [31,32], the main idea of the BE-SBS method, which takes into account Krylov iterative solvers, is to get the global response for a problem working exclusively with its local full-populated subsystems of equations, which are independently generated and stored. No global explicit system matrix is assembled; no zero blocks are stored or handled. The boundary conditions for the $i$th subdomain (associated with the outer boundary of $\Omega_i$, denoted by $\Gamma_{ii}$) are introduced during the matrix assembly for each subsystem. The interface conditions, e.g. at the interface $\Gamma_{ij}$ (between the subdomains $i$ and $j$), given by

$$\left\{\begin{array}{l}\mathbf{u}_{ij}=\mathbf{u}_{ji}\\ \mathbf{p}_{ij}=-\mathbf{p}_{ji}\end{array}\right. \text{at } \Gamma_{ij} \tag{2}$$

are directly (not iteratively) imposed while calculating the matrix–vector products during the iterative solution process, where $\mathbf{u}_{ij}$ and $\mathbf{p}_{ij}$ denote, respectively, the displacement and traction vectors of subdomain $i$ at $\Gamma_{ij}$. Thus, for $n_s$ subregions, after introducing the boundary conditions, the BE global system of equations is then given by

$$\sum_{m=1}^{i-1}(\mathbf{H}_{im}\mathbf{u}_{mi}-\mathbf{G}_{im}\mathbf{p}_{im})+\mathbf{A}_{ii}\mathbf{x}_i+\sum_{m=i+1}^{n_s}(\mathbf{H}_{im}\mathbf{u}_{im}+\mathbf{G}_{im}\mathbf{p}_{mi})=\mathbf{B}_{ii}\mathbf{y}_i,\ i=1,n_s, \tag{3}$$

where $\mathbf{A}_{ii}$, $\mathbf{B}_{ii}$, $\mathbf{H}_{ij}$ and $\mathbf{G}_{ij}$ denote the regular BE matrices obtained for source points pertaining to subregion $\Omega_i$ and associated, respectively, with the boundary vectors $\mathbf{x}_i$, $\mathbf{y}_i$, $\mathbf{u}_{ij}$ and $\mathbf{p}_{ij}$. Note that $\mathbf{x}_i$ and $\mathbf{y}_i$ are the vectors containing the boundary unknown and boundary prescribed values of $\Omega_i$ (after column interchange).

To accelerate the solver iterations, structured matrix–vector products (SMVP) [21,28] are employed. Herein, the matrix columns of a given subregion are grouped into three separate blocks: one associated with interfaces $\Gamma_{ij}$ for which $i>j$, a second associated with the outer boundary $\Gamma_{ii}$, at which boundary values are prescribed, and one associated with interfaces $\Gamma_{ij}$ for $i<j$. This corresponds to the matrix structuring given in (4) below

$$\begin{array}{lllll} & \text{block 1} & \text{block 2} & \text{block 3} & \\ \mathbf{H}_i = [ & \mathbf{H}_{i1}\ \cdots\ \mathbf{H}_{i,i-1} & \mathbf{A}_{ii} & \mathbf{H}_{i,i+1}\ \cdots\ \mathbf{H}_{in} & ] \\ \mathbf{G}_i = [ & \mathbf{G}_{i1}\ \cdots\ \mathbf{G}_{i,i-1} & \mathbf{B}_{ii} & \mathbf{G}_{i,i+1}\ \cdots\ \mathbf{G}_{in} & ] \end{array} \tag{4}$$

$\mathbf{H}_i$ and $\mathbf{G}_i$ are the BE matrices for the $i$th subregion.

Notice that the 3D BE subregion-by-subregion algorithm discussed in this section is a general-purpose technique for the BEM analysis of multi-domain problems with a generic number of subregions, of any shapes, under any spatial substructure arrangements (periodic or non-periodic). As easily inferred, the non-linear contact can also be promptly incorporated into the algorithm.

## 3. BE-SBS-based block-diagonal preconditioning

If the system of equations in (3) were, say for $n_s=4$ (four subregions), explicitly assembled, it would have the following general aspect:

$$\begin{array}{c|cccc|cccc|cccc|cccc|} & \multicolumn{4}{c|}{\Omega_1} & \multicolumn{4}{c|}{\Omega_2} & \multicolumn{4}{c|}{\Omega_3} & \multicolumn{4}{c|}{\Omega_4} \\ \hline \Omega_1 & \mathbf{A}_{11} & \mathbf{H}_{12} & \mathbf{H}_{13} & \mathbf{H}_{14} & \mathbf{G}_{12} & & & & \mathbf{G}_{13} & & & & \mathbf{G}_{14} & & & \\ \Omega_2 & & \mathbf{H}_{21} & & & -\mathbf{G}_{21} & \mathbf{A}_{22} & \mathbf{H}_{23} & \mathbf{H}_{24} & & \mathbf{G}_{23} & & & & \mathbf{G}_{24} & & \\ \Omega_3 & & & \mathbf{H}_{31} & & & & \mathbf{H}_{32} & & -\mathbf{G}_{31} & -\mathbf{G}_{32} & \mathbf{A}_{33} & \mathbf{H}_{34} & & & \mathbf{G}_{34} & \\ \Omega_4 & & & & \mathbf{H}_{41} & & & & \mathbf{H}_{42} & & & & \mathbf{H}_{43} & -\mathbf{G}_{41} & -\mathbf{G}_{42} & -\mathbf{G}_{43} & \mathbf{A}_{44} \\ \hline \end{array} \begin{bmatrix} \mathbf{x}_{11}\\ \mathbf{u}_{12}\\ \mathbf{u}_{13}\\ \mathbf{u}_{14}\\ \mathbf{p}_{21}\\ \mathbf{x}_{22}\\ \mathbf{u}_{23}\\ \mathbf{u}_{24}\\ \mathbf{p}_{31}\\ \mathbf{p}_{32}\\ \mathbf{x}_{33}\\ \mathbf{u}_{34}\\ \mathbf{p}_{41}\\ \mathbf{p}_{42}\\ \mathbf{p}_{43}\\ \mathbf{x}_{44} \end{bmatrix}$$

$$= \begin{array}{|cccc|} \Omega_1 & \Omega_2 & \Omega_3 & \Omega_4 \\ \hline \mathbf{B}_{11} & & & \\ & \mathbf{B}_{22} & & \\ & & \mathbf{B}_{33} & \\ & & & \mathbf{B}_{44} \\ \hline \end{array} \begin{bmatrix} \mathbf{y}_1\\ \mathbf{y}_2\\ \mathbf{y}_3\\ \mathbf{y}_4 \end{bmatrix} \begin{array}{c} \Omega_1\\ \Omega_2\\ \Omega_3\\ \Omega_4 \end{array} \tag{5}$$

In this system, note that if the $i$th and $j$th subdomains are not coupled, so the respective block matrices are identically null, i.e. $\mathbf{H}_{ij}=\mathbf{H}_{ji}=\mathbf{G}_{ij}=\mathbf{G}_{ji}=\mathbf{0}$. However, as commented previously, we do not have any explicit system of equations. Instead, the working subsystems are those (structured) ones shown in expression (4). The matrix–vector and transpose-matrix–vector products are then calculated from the separate contributions from each subsystem, and during the solver iterations, the interface conditions are imposed in a direct way.

In this study, the preconditioner is constructed by taking the diagonal blocks of the coupled system. Based on the particular (explicit) system of equations shown in (5), we are talking about that subset of positions highlighted in gray. Inferring from Eq. (5) that, for a generic number of subregions, the diagonal blocks of the coupled system are given by

$$\mathbf{Q}_i=\begin{bmatrix}-\mathbf{G}_{i1} & \cdots & -\mathbf{G}_{i,i-1} & \mathbf{A}_{ii} & \mathbf{H}_{i,i+1} & \cdots & \mathbf{H}_{in}\end{bmatrix},\ i=1,\ n_s, \tag{6}$$

where the $\mathbf{Q}_i$ matrices are straightforwardly formed having the subregion matrices of the model at hand, the construction of the global SBS-based block-diagonal preconditioner for the coupled system of Eq. (3) is then immediate. Explicitly written, this global preconditioner is of the form

$$\mathbf{Q}=\begin{bmatrix}\mathbf{Q}_1 & & & & \\ & \ddots & & & \\ & & \mathbf{Q}_i & & \\ & & & \ddots & \\ & & & & \mathbf{Q}_{n_s}\end{bmatrix} \tag{7}$$

However, as the subdomain submatrices, this global preconditioner is not explicitly assembled either; it is separately stored per subregion at an additional memory space of the size $[nno(is)\times ndofn]\times[nno(is)\times ndofn]$, where $nno(is)$ is the number of nodes of the $is$th subregion, and $ndofn$ is the number of degrees of freedom per node (the same for the whole model). In the computational implementation, only their **L** and **U** decomposition factors, obtained right after the BE subsystem matrices are formed, are stored. In this work, the Bi-CG solver, which also requires transpose matrix–vector multiplications, is employed. In effect, by considering left preconditioning, the preconditioner is applied to the iterative solution for the $i$th subregion, $\boldsymbol{x}_i$, by solving systems like $(\mathbf{L}_i\mathbf{U}_i)\mathbf{x}_i=\mathbf{x}_i$ and $(\mathbf{L}_i\mathbf{U}_i)^T\mathbf{x}_i=\mathbf{x}_i$. Notice that the irregular convergence property of the Bi-CG iterations actually highlights the importance and efficiency of the preconditioner.

## 4. Results and discussions

The efficiency of the SBS-based block-diagonal preconditioner detailed above is observed by determining engineering constants for complex CNT-based composites. The composite representative volume elements (RVEs) are constructed by arranging long and short CNT fibers along square and hexagonal packing patterns inside the polymer matrix. A single or several coupled composite unit cells have been used.

The integration quadratures employed in the analyses follow the general description in Section 2 above. In all analyses, 8 × 8 and 6 integration points are used for evaluating all surface and line integrals involved, respectively. In all RVEs, the following pure phase constants are adopted [33]:

$$\text{CNT}: E_{CNT}=1000\frac{nN}{nm^2}(\text{GPa});\ \nu_{CNT}=0.30,$$

$$\text{Matrix}: E_m=100\frac{nN}{nm^2}(\text{GPa});\ \nu_m=0.30.$$

The long CNT fibers are geometrically defined by cylindrical tubes having outer radius $r_0=5.0$ nm and inner radius $r_i=4.6$ nm, and length $l_f=10$ nm. The short CNTs have cross section and hemispherical caps with same previous outer and inner radius; its length (including both caps) is $l_f=50$ nm. Noting that long-fiber composites have their fibers all the way through their length, 2D elasticity description applies, and so, the fiber lengths in 3D models must not necessarily be long at all. Thus, in the 3D models in this paper, the long CNTs ($l_f=10$ nm) are actually shorter than the short CNTs ($l_f=50$ nm).

In general, when needed, discontinuous boundary elements are automatically generated by shifting the nodes interior to the elements a distance of $d=0.10$ (measured in the natural coordinate system). The matrix-copy option is also conveniently considered to replicate physically and geometrically identical subdomains, avoiding then assembling repeatedly their corresponding matrices. The 8-node quadrilateral boundary element is employed, and the tolerance for the iterative solver (Bi-CG) is taken as $\zeta=10^{-8}$. The diagonal preconditioning (Jacobi) and the preconditioning proposed in this paper (BE-SBS-based block-diagonal decomposition) are then contrasted to show the efficiency brought about by the latter preconditioner. The analyses were carried out at a notebook with dual intel 2.26 GHz processor, and 3 GB of random access memory.

### 4.1. RVEs with square-packed long CNT fibers

In this application, RVEs based on 1 × 1, 2 × 2, and 5 × 5 unit cells are employed for modeling long-CNT-based composites (see Fig. 2). The length along the 1 direction (fiber direction) of the specimen is the same as the CNT length ($l_1=10$ nm). The other dimensions of each unit cell (along the 2 and 3 axes; see Fig. 2) are taken as $l_2=l_3=20$ nm. Important model data are provided in Table 1. In Table 2, the engineering parameters extracted from the analysis of all the RVEs shown in Fig. 2 are compared with results calculated by Liu and Chen [33] via finite-element analysis, and estimated (when possible) by the rules of mixture (see Refs. [33, 34]).

**Table 1**
Model data for the square-packed long-CNT RVEs.

| Model | *nsub*[a] | *nel*[b] | *nnodes*[c] | *ndof* [d] | Sparsity (%) |
|---|---|---|---|---|---|
| 1 × 1 | 2 | 128 | 608 | 1824 | 29 |
| 2 × 2 | 8 | 512 | 2660 | 7980 | 81 |
| 5 × 5 | 50 | 1344 | 17,456 | 52,368 | 97 |

[a] n. of subregions
[b] n. of elements
[c] n. of nodes
[d] n. of degrees of freedom

**Table 2**
Engineering constants for the square-packed long-CNT RVEs.

| Model | $E_1/E_m$ | $E_2/E_m$, $E_3/E_m$ | $\nu_{12}$,$\nu_{13}$ | $\nu_{23}$ |
|---|---|---|---|---|
| 1 × 1 | 1.3227 | 0.8302 | 0.2974 | 0.3595 |
| 2 × 2 | 1.3228 | 0.8319 | 0.2973 | 0.3600 |
| 5 × 5 | 1.3228 | 0.8319 | 0.2972 | 0.3580 |
| Chen & Liu (3D FE) | 1.3255 | 0.8492 | 0.3000 | 0.3799 |
| Rule of mixture[a] | 1.3255 | – | – | – |

[a] RVE volume fraction is $V_f$=3.617%.

As seen from Table 2, there is a very good agreement between the material parameters calculated with the present method and estimated by refined 3D FE models [33] or the rules of mixture ([22, 34]). Furthermore, no significant change in the constant values is also observed as the number of unit cells per RVE increases.

In Table 3, results showing the performance of the preconditioners are presented. As one sees, compared to the Jacobi preconditioner, a considerable acceleration of Bi-CG solver is observed when the BE SBS-based block-diagonal one is applied (e.g. it makes the solver about 24 times faster for the 5 × 5-unit-cell RVE under strain state 1). Notice that, although the cost per iteration is higher using the BE SBS-based block-diagonal preconditioning, the corresponding number of iterations is considerably reduced. The decaying of the Euclidean residual norm, $\|\boldsymbol{\delta}\|_2$, as a function of the iteration order for both contrasted preconditioners is also shown in Fig. 3. This graph clearly shows the superiority of the BE SBS-based block-diagonal preconditioning.

### 4.2. RVEs with hexagonal-packed long CNT fibers

Here, 1 × 1, 2 × 2, 3 × 3, and 5 × 5 RVEs are analyzed (see Fig. 4), each one built with unit cells having dimensions $l_1 = 10$ nm and $l_2 = l_3 = 20$ nm. Model data and estimated material parameters are given in Tables 4 and 5, respectively. For comparison purposes, only $E_1$, estimated by the rules of mixture, is considered [34], and we verify that $E_1$ values estimated by the rules of mixture and calculated with the present method are about the same magnitude. Here we also note that increasing the number of unit cells per RVE does not significantly change the estimated material constants. In Table 6 the performance of both preconditioners is presented, and in the graph in Fig. 5 the decaying of the corresponding residual Euclidean norms during the Bi-CG iterations is given. Again, the performance of the BE SBS-based block-diagonal preconditioning has shown superior.

### 4.3. RVEs with squared-packed short CNT fibers

In this application, the RVEs are constituted of 1 × 1 and 2 × 2 short capsule-like CNTs smeared inside the matrix material along square-packing patterns (Fig. 6, Table 7). A single-cell RVE has outer dimensions $l_1 = 100$ nm and $l_2 = l_3 = 20$ nm, and the geometrical details of the CNT were furnished above. Compared to the results obtained by Liu and Chen [33], and, when possible, by the extended rule of mixture [22], the values estimated by applying the BE SBS-based strategy show good agreement (Table 8). For both RVEs, about the same material constant values are estimated. In Table 9, performance data of the Jacobi and BE SBS-based preconditioners are given. In Fig. 7, the residual norm decaying as a function of the iteration order is shown. Again, the BE SBS-based preconditioning clearly increases the efficiency of the Bi-CG solver, making it for the 2 × 2-unit-cell RVE under strain state 1 about 10 times faster.

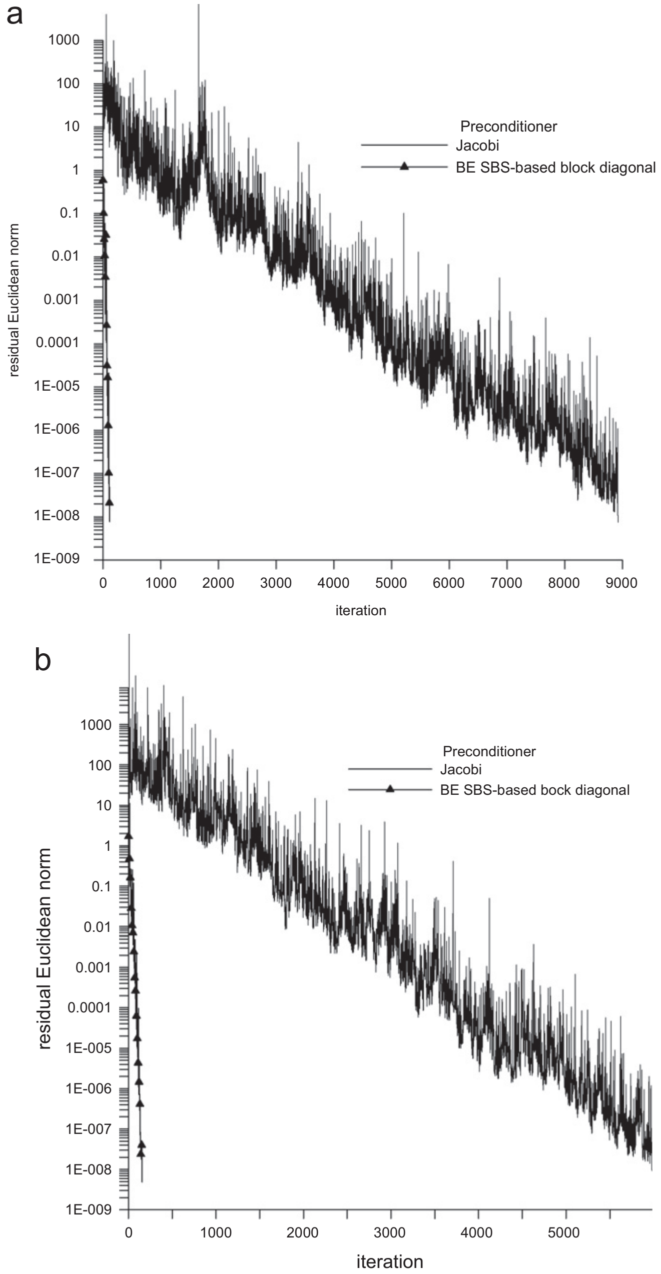

**Fig. 3.** Residual norm vs. iteration: 5 × 5-unit-cell, square-packed long CNT: (a) strain state 1 and (b) strain state 2.

**Table 3**
Performance data for the square-packed long-CNT RVEs; tol = $1.0 \times 10^{-8}$.

| Model | System order | n. of iterations (BE SBS-based block diagonal) | n. of iterations (Jacobi) | CPU time (*s*) (BE SBS-based block diagonal)[a] | CPU time (*s*) (Jacobi) |
|---|---|---|---|---|---|
| 1 × 1 unit cell, strain state 1 | 1824 | 57 | 561 | 2 | 5 |
| 1 × 1 unit cell, strain state 2 | 1824 | 73 | 621 | 2 | 6 |
| 2 × 2 unit cells, strain state 1 | 7980 | 81 | 2241 | 11 | 104 |
| 2 × 2 unit cells, strain state 2 | 7980 | 104 | 1805 | 12 | 84 |
| 5 × 5 unit cells, strain state 1 | 52,368 | 116 | 8920 | 119 | 2917 |
| 5 × 5 unit cells, strain state 2 | 52,368 | 157 | 5983 | 142 | 2,084 |

[a] Including the LU decomposition CPU time

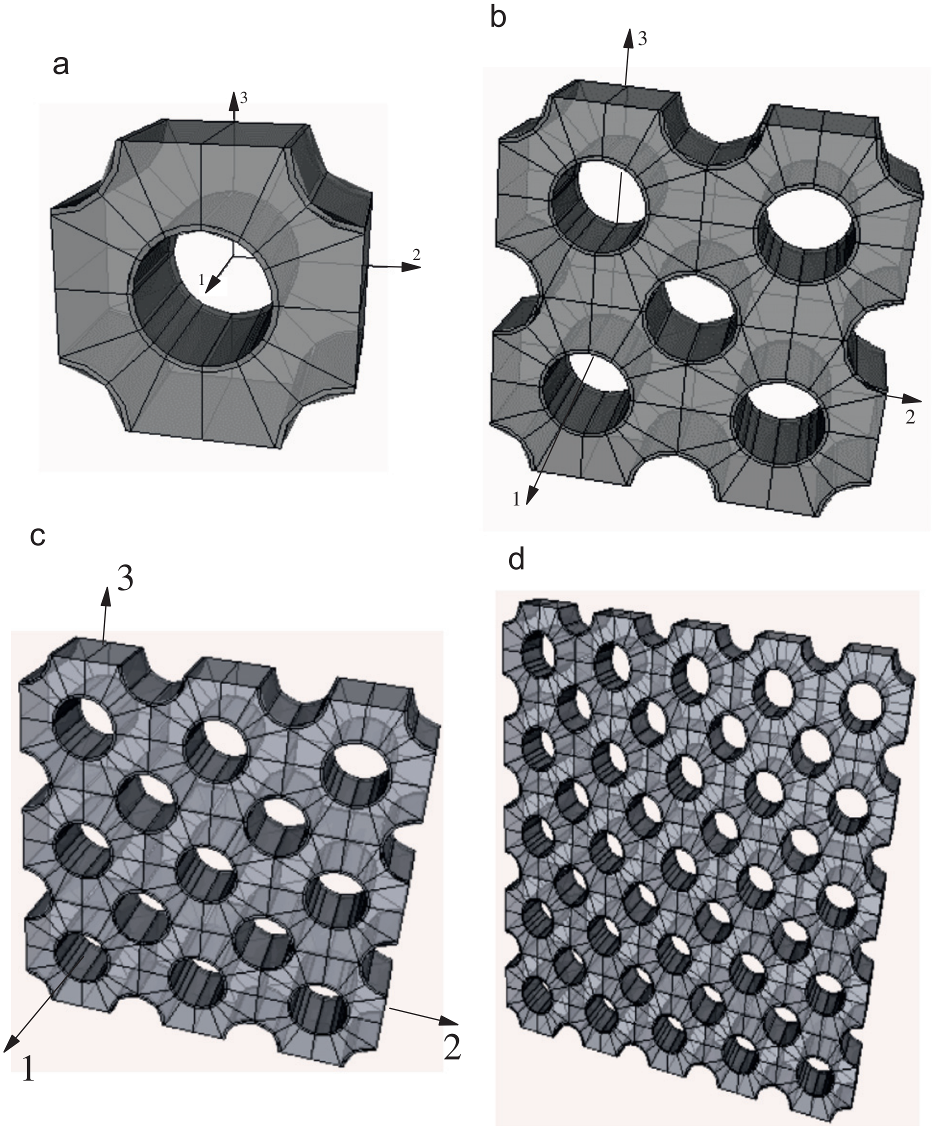

**Fig. 4.** Hexagonal-packed long-CNT-based RVEs.

**Table 4**
Model data for the hexagonal-packed long-CNT RVEs.

| Model | *nsub*[a] | *nel*[b] | *nnodes*[c] | *ndof*[d] | Sparsity (%) |
|---|---|---|---|---|---|
| 1 × 1 | 6 | 138 | 856 | 2568 | 72 |
| 2 × 2 | 17 | 656 | 3456 | 10,368 | 86 |
| 3 × 3 | 34 | 1464 | 7800 | 23,400 | 93 |
| 5 × 5 | 86 | 4040 | 21,720 | 65,160 | 97 |

[a] n. of subregions
[b] n. of elements
[c] n. of functional nodes
[d] n. of degrees of freedom

**Table 5**
Engineering constants for the hexagonal-packed long-CNT RVE.

| Model | $E_1/E_m$ | $E_2E_m$, $E_3/E_m$ | $\nu_{12}$,$\nu_{13}$ | $\nu_{23}$ |
|---|---|---|---|---|
| 1 × 1 | 1.8081 | 1.0889 | 0.2943 | 0.5107 |
| 2 × 2 | 1.8074 | 1.0839 | 0.2936 | 0.5107 |
| 3 × 3 | 1.8074 | 1.0916 | 0.2931 | 0.5185 |
| 5 × 5 | 1.8126 | 1.0813 | 0.2927 | 0.4997 |
| Rule of mixture[a] | 1.8131 | – | – | – |

[a] RVE volume fraction is $V_f$=9.035%.

## 5. Conclusions and prospects

Using a robust boundary-element subregion-by-subregion (BE SBS) technique proposed in previous papers ([21, 35]), a straightforward strategy for constructing block-diagonal preconditioners for BE systems of equations is presented. The performance of this preconditioning was verified by analyzing complex composite representative volume elements (RVEs).

Observing Tables 3, 6 and 9, and graphs in Figs. 3, 5 and 7, we see that the BE-SBS-based block-diagonal preconditioning, compared to the Jacobi (diagonal) one, considerably accelerates the Bi-CG solver, making it in all cases analyzed several times faster. Moreover, it causes the decaying of the residual Euclidean norm as a function of the iteration order to be more regular (see Figs. 3, 5 and 7). In fact, the BE-SBS-based block-diagonal preconditioning states a transition (or connection) between direct and iterative solvers, in the sense that the less the number of interfaces, the closer to the global system matrix the preconditioning

**Table 6**
Performance data for the hexagonal-packed long-CNT RVEs; tol$=1.0\times10^{-8}$.

| Model | System order | n. of iterations (BE SBS-based block diagonal) | n. of iterations (Jacobi) | CPU time ($s$) (BE SBS-based block diagonal)[a] | CPU time ($s$) (Jacobi) |
|---|---|---|---|---|---|
| 1 × 1 unit cell, strain state 1 | 2568 | 68 | 446 | 3 | 5 |
| 1 × 1 unit cell, strain state 2 | 2568 | 85 | 451 | 3 | 5 |
| 2 × 2 unit cells, strain state 1 | 10,368 | 249 | 1170 | 29 | 64 |
| 2 × 2 unit cells, strain state 2 | 10,368 | 296 | 1166 | 33 | 64 |
| 3 × 3 unit cells, strain state 1 | 23,400 | 316 | 1696 | 79 | 211 |
| 3 × 3 unit cells, strain state 2 | 23,400 | 477 | 2413 | 114 | 297 |
| 5 × 5 unit cells, strain state 1 | 65,160 | 614 | 4537 | 490 | 1713 |
| 5 × 5 unit cells, strain state 2 | 65,160 | 884 | 4058 | 565 | 1476 |

[a] Including the LU decomposition CPU time

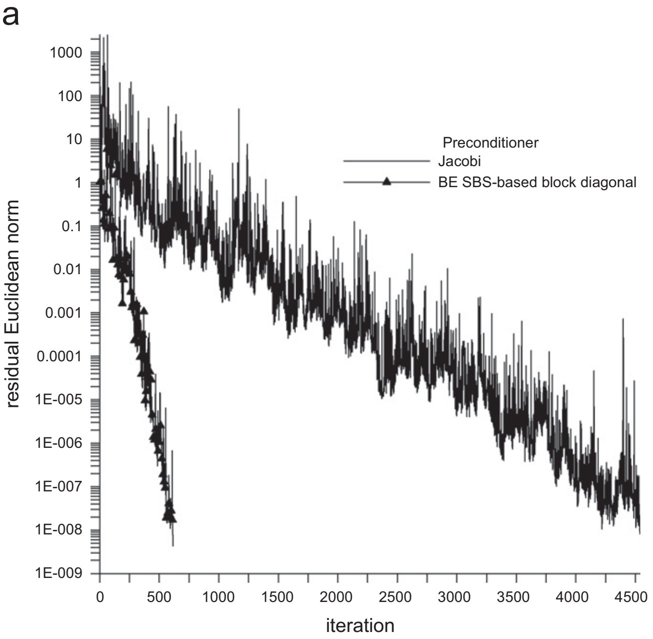

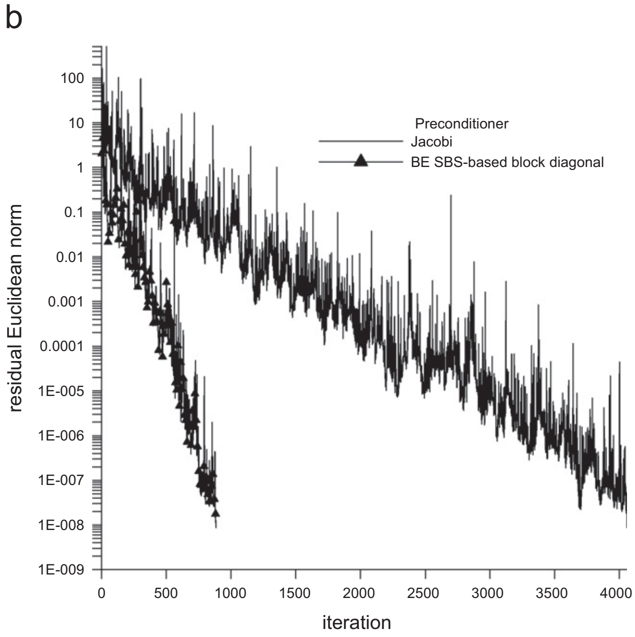

**Fig. 5.** Residual norm vs. iteration: 5 × 5-unit-cell, hexagonal-packed long CNT: (a) strain state 1 and (b) strain state 2.

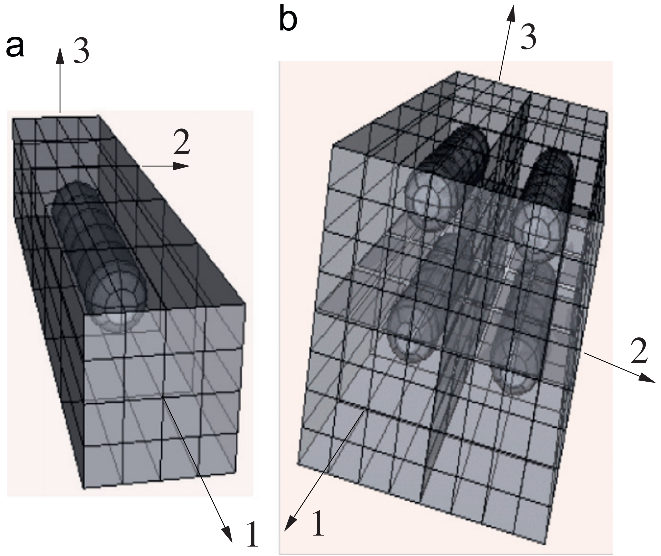

**Fig. 6.** Square-packed short-CNT-based RVEs.

**Table 7**
Model data for the square-packed short-CNT RVEs.

| Model | *nsub*[a] | *nel*[b] | *nnodes*[c] | *ndof* [d] | Sparsity (%) |
|---|---|---|---|---|---|
| 1 × 1 | 2 | 352 | 1064 | 3192 | 27 |
| 2 × 2 | 8 | 1408 | 5156 | 15,468 | 78 |

[a] n. of subregions
[b] n. of elements
[c] n. of functional nodes
[d] n. of degrees of freedom

**Table 8**
Engineering constants for the square-packed short-CNT RVEs.

| Model | $E_1/E_m$ | $E_2/E_m$, $E_3/E_m$ | $\nu_{12}$,$\nu_{13}$ | $\nu_{23}$ |
|---|---|---|---|---|
| 1 × 1 | 1.0378 | 0.9366 | 0.2963 | 0.3207 |
| 2 × 2 | 1.0379 | 0.9379 | 0.2976 | 0.3217 |
| Chen & Liu (3D FE) | 1.0391 | 0.9342 | 0.3009 | 0.3217 |
| Rule of mixture[a] | 1.0396 | – | – | – |

[a] The extended rule of mixture is considered.

matrix, **Q**, is. For example, if no interface is present in the model, the **Q** matrix is identical to the system matrix (with one single or many decoupled subregions), and convergence will be reached at one

**Table 9**
Performance data for square-packed short-CNT RVEs; tol $=1.0\times10^{-8}$.

| Model | System order | n. of iterations (BE SBS-based block diagonal) | n. of iterations (Jacobi) | CPU time (*s*) (BE SBS-based block diagonal)[a] | CPU time (*s*) (Jacobi) |
|---|---|---|---|---|---|
| 1 × 1 unit cell, strain state 1 | 3192 | 51 | 763 | 6 | 21 |
| 1 × 1 unit cell, strain state 2 | 3192 | 67 | 822 | 7 | 23 |
| 2 × 2 unit cells, strain state 1 | 15,468 | 83 | 2348 | 60 | 610 |
| 2 × 2 unit cells, strain state 2 | 15,468 | 87 | 2510 | 60 | 481 |

[a] Including the LU decomposition CPU time.

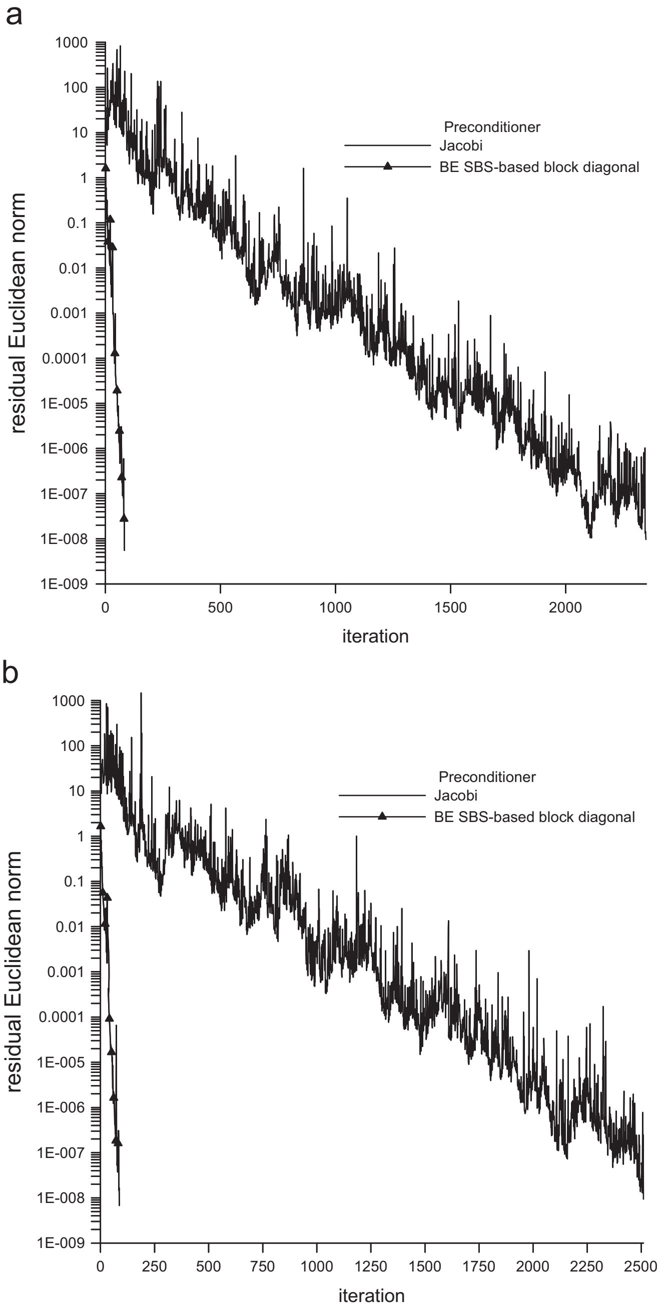

**Fig. 7.** Residual norm vs. iteration: 2 × 2-unit-cells, square-packed short CNT: (a) strain state 1 and (b) strain state 2.

single iteration. In addition, knowing that the global coupled system is highly sparse, we can well conclude that the preconditioner proposed will be certainly a good approximation of the global system matrix, which is one of the requirements for finding good preconditioners. Generally speaking, the larger the size of the subsystems, the higher the cost for constructing the preconditioner, however, on the other hand, a better approximation for the global system is achieved, reducing then the number of iterations. Furthermore, being this preconditioner based on the BE-SBS algorithm, its parallelization is immediate. By the way, in a cost-benefit analysis, not only the acceleration of the iterative process but also the solver-convergence reliability and parallel-processing suitability should be considered as benefit.

Among others, we can finally affirm that the BE-SBS strategy has the following general advantages: (1) it is a fundamental technique to model complex heterogeneous problems, (2) it is a spontaneous way to parallelize BE codes [36], and (3) it is, as shown in this paper, an easy way to construct efficient block-diagonal preconditioners for the Krylov solver the BE-SBS algorithm itself embeds. Although reliable and fast convergence of iterative solvers is a still open question for general practical modeling in engineering, mainly in the case of BE formulations, where usually non-symmetric matrices are involved [37], it seems that the BE-SBS-based block-diagonal preconditioner proposed in this paper will be one more contribution towards making the reliable use of iterative solvers in engineering feasible. Of course, much more efficiency would have been attained if, compared to the Bi-CG solver, more efficient Krylov solvers, as e.g. the Bi-CGSTAB(*l*) [8] or the GPBi-CG [15], had been employed.

## Acknowledgements

This research was sponsored by the Office of Advanced Scientific Computing Research, U.S. Department of Energy under Contract DE-AC05-00OR22725 with UT-Battelle, LLC, the Brazilian Research Council (CNPq), and by the Research Foundation for the State of Minas Gerais (FAPEMIG), Brazil.

## References

[1] van der Vorst HA. Iterative Krylov Methods for Large Linear Systems. Cambridge University Press; 2003.
[2] Saad Y. Iterative Methods for Sparse Linear Systems, Society for Industrial and Applied Mathematics. Philadelphia: SIAM; 2003.
[3] Lanczos C. Solution of systems of linear equations by minimized iteration. J Res Nat Bur Stand 1952;49:33–53.
[4] Fletcher R. Conjugate gradient methods for indefinite systems, Lecture Notes in Mathematics 506. Berlin: Spriger-Verlag; 1976.
[5] Saad Y, Schultz MH. GMRES: a generalized minimum residual algorithm for solving nonsymmetric linear systems. SIAM J Sci Stat Comput 1986;7:856–69.
[6] Sonneveld P. CGS, a fast Lanczos-type solver for nonsymetric linear systems. SIAM J Sci Stat Comput 1989;10:36–52.
[7] van der Vorst HA. Bi-CGSTAB: a fast and smoothly converging variant of Bi-CG for the solution of nonsymmetric linear systems. SIAM J Sci Stat Comput 1992;13:631–44.
[8] Sleijpen GLG, Fokkema DR. BICGSTAB(*L*) for linear equations involving unsymmetric matrices with complex spectrum. Electron Trans Num Methods Anal 1993;1:11–32.
[9] Araújo FC, Mansur WJ. Iterative solvers for BEM systems of equations. In: Proceedings of the 11th International Conference on Boundary Element Methods, Cambridge, USA, 1989, vol. 1, pp. 263–274.

[10] Araújo FC, Mansur WJ, Malaghini JEB. Biconjugate gradient acceleration for large BEM systems of equations In: Proceedings of the 12th International Conference on Boundary Element Methods, Sapporo, Japan, vol. 1, 1990, pp. 99–110.

[11] Kane JH, Keyes DE, Prasad KG. Iterative equation solution techniques in boundary element analysis. Int J Numer Methods Eng 1991;31:1511–36.

[12] Mansur WJ, Araújo FC, Malaghini JEB. Solution of BEM systems of equations via iterative techniques. Int J Numer Methods Eng 1992;33:1823–41.

[13] Bettess JA. Economical solution techniques for boundary integral matrices. Int J Numer Methods Eng 1983;19:1073–7.

[14] Mullen RL, Rencis JJ. Iterative methods for solving boundary element equations. Comput Struct 1987;25:713–23.

[15] Zhang S-L. A class of product-type Krylov-subspace methods for solving nonsymmetric linear systems. J Comp Appl Math 2002;149:297–305.

[16] Vavasis SA. Preconditioning for boundary integral-equations. SIAM J Matrix Anal Appl 1992;13:905–25.

[17] Chen K. Matrix Preconditioning Techniques and Applications. Cambridge, UK: Cambridge University Press; 2005.

[18] Davey K, Bounds S. A preconditioning strategy for the solution of linear boundary element systems using the GMRES method. Appl Numer Math 1997;23:443–56.

[19] Merkel M, Bulgakov V, Bialecki R, Kuhn G. Iterative solution of large-scale 3D-BEM industrial problems. Eng Anal Boundary Elem 1998;22:183–97.

[20] Chen K. On a class of preconditioning methods for dense linear systems from boundary elements. SIAM J Sci Comput 1998;20:684–98.

[21] Araújo FC, Silva KI, Telles JCF. Generic domain decomposition and iterative solvers for 3D BEM problems. Int J Numer Methods Eng 2006;68:448–72.

[22] Araújo FC, Gray LJ. Evaluation of effective material parameters of CNT-reinforced composites via 3D BEM. Comp Mod Eng Sci 2008;24(2):103–21.

[23] Araújo FC, Dors C, Martins CJ, Mansur WJ. New developments on BE/BE multi–zone algorithms based on Krylov solvers—applications to 3D frequency-dependent problems. J Braz Soc Mech Sci Eng 2004;26(2):231–48.

[24] Li HB, Han GM, Mang HA. A new method for evaluating for evaluating singular integrals in stress analysis of solids by the direct boundary element method. Int J Numer Methods Eng 1985;21:2071–98.

[25] Telles JCF. A self-adaptive co-ordinate transformation for efficient numerical evaluation of general boundary element integrals. Int J Numer Methods Eng 1987;24:959–73.

[26] Liu Y. Analysis of shell-like structures by the boundary element method based on 3-D elasticity: formulation and verification. Int J Numer Methods Eng 1998;41:541–58.

[27] Chen XL, Liu YJ. An advanced 3D boundary element method for characterization of composite materials. Eng Anal Boundary Elem 2005;29:513–23.

[28] Araújo FC, Gray LJ. Analysis of thin-walled structural elements via 3D standard BEM with generic substructuring. Comput Mech 2008;41:633–45.

[29] Hughes TJR, Levit I, Winget L. An element-by-element solution algorithm for problems of structural and solid mechanics. Comput Methods Appl Mech Eng 1983;36(2):241–54.

[30] Farhat C, Roux F-X. An unconventional domain decomposition method for an efficient parallel solution of large-scale finite element systems. SIAM J Sci Stat Comput 1992;13:379–96.

[31] Araujo FC, Belmonte GJ, Freitas MSR. Efficiency increment in 3D multizone boundary element algorithms by use of iterative solvers. J Chin Inst Eng 2000;23(3):269–74.

[32] Yu W, Wang Z, Hong X. Preconditioned multi-zone boundary element analysis for fast 3D electric simulation. Eng Anal Boundary Elem 2004;28(9):1035–44.

[33] Chen XL, Liu YJ. Square representative volume elements for evaluating the effective material properties of carbon nanotube-based composites. Comput Mater Sci 2004;29:1–11.

[34] Hyer MW. Stress Analysis of Fiber-Reinforced Composite Materials. 1st ed.. Boston: McGraw-Hill; 1998.

[35] Araújo FC, Silva KI, Telles JCF. Application of a generic domain-decomposition strategy to solve shell-like problems through 3D BE models. Commun Numer Methods Eng 2007;23:771–85.

[36] Araújo FC, d'Azevedo EF, Gray LJ. Boundary-element parallel-computing algorithm for the microstructural analysis of general composites. Comput Struct 2010;88:773–84.

[37] Barrett R, Berry M, Dongarra J, Eijkhout V, Romine C. Algorithmic bombardment for the iterative solution of linear systems: a poly-iterative approach. J Comp Appl Math 1996;74:91–109.